COINCIDENCE MEASUREMENT OF THE REACTION $^{56}Fe+p$ AT *1 GeV* PER NUCLEON WITH SPALADIN

Jean-Éric Ducret *et al.*

DSM/DAPNIA/Service de Physique Nucléaire, CEA-Saclay, F91191 GIF sur Yvette, France
jean-eric.ducret@cea.fr

The SPALADIN experiment using the inverse-kinematics technique where the heavy-ion beam is sent onto a liquid-hydrogen target has been carried-out at GSI (Darmstadt, Germany) in order to study the spallation of ^{56}Fe. On an event-by-event basis, spallation residues, light-charged particles and neutrons were detected in coincidence. The combination of the inverse kinematics and of the acceptance of the set-up focuses the measurement on the low centre-of-mass energy fragments of the reaction essentially originating from the de-excitation of the prefragment formed at the end of the intranuclear cascade. Preliminary results of the coincidence data taken at 1 GeV per nucleon are presented and compared to theoretical calculations. We emphasize on the evolution with the excitation energy of the reaction of the average particle and fragment multiplicities as well as on multi-fragment events.

I. INTRODUCTION

I.A. Motivations

Spallation can be defined as the reaction of an atomic nucleus with a proton of a few 100 *MeV* in the centre-of-mass frame and is at a meeting point between basic and applied nuclear physics. On the one hand, understanding the spallation mechanism is a necessary step when building theoretical models to describe quantitatively ion-ion reactions in the *GeV* range. Indeed, the spallation mechanism is relatively simple because of the basic features of spallation: Relatively low compression effects related to an essentially thermal excitation of the target nucleus, along with mainly one hot source of low-energy fragments and particles, and rather low values of the angular momentum of the excited nucleus which limit the influence of centrifugal forces on the reaction dynamics. On the other hand, spallation is at the basis of the design of accelerator-driven systems (ADS) or the production of radioactive-ion beams. It is also the basic reaction to be modelled in the study of the damages produced by cosmic rays on electronics embarked on satellites and spacecrafts. The understanding of spallation is therefore of great importance, especially in order to produce event generators based on physics models to be implemented in global simulations of complex systems, as those quoted above, in which spallation plays a major role.

We present here the first results of the experiment SPALADIN[1], designed to study in detail the reaction $^{56}Fe + p$ at 1 *GeV* per nucleon kinetic energy. ^{56}Fe was chosen for three reasons: 1) it is the main structural component of ADS, in particular for the vacuum window in between the target and the proton accelerator; 2) spallation of ^{56}Fe at 1 *GeV* allows to produce relatively excited nuclei (a few percents of the total cross-section above 5 MeV per nucleon of excitation energy which is considered in the literature as the threshold for the multifragmentation of excited nuclear systems) which permits to probe a wide range of de-excitation mechanisms to test theoretical models; 3) the final states produced in the spallation of this nucleus are well within the capabilities of the SPALADIN experimental set-up in order to assure a good detection of the multiplicities and a clear identification of the different species.

The description of spallation is based on a two-step model: 1) an intranuclear cascade (INC) leading to the formation of a highly excited nucleus (the prefragment); 2) the prefragment decay. The INC corresponds to the first instants of the spallation reaction when, in the centre-of-mass, the incoming proton collides with individual nucleons of the target nucleus. These nucleons, which have acquired momentum in the first collision, can collide, afterwards, with other nucleons inside the nucleus. The INC leads rapidly (a few 10 *fm/c*) to the formation of an excited system, the prefragment, which has lost the memory of the entrance channel kinematics. In the analysis presented here, we have used INCL4 of Ref.[2] to describe the INC. In the two-step model, the assumption is made that the prefragment is in statistical equilibrium. Its decay is described therefore by statistical models which include different channels such as light-particle emission (evaporation), asymmetric splitting in composite fragments, and fission for the heavy nuclei, or even multifragmentation. In the present study, four

models to describe the de-excitation of the prefragment have been used: ABLA[3], GEM[4], GEMINI[5] and SMM[6]. ABLA computes the Weisskopf-Ewing evaporation of light particles (*n*, *p* and ^{4}He) and comprises an accurate model of fission for the heavy nuclei, GEM is essentially a generalization of the Weisskopf-Ewing evaporation to the production of intermediate-mass fragments (IMP) up to ^{24}Mg. GEMINI models the production of *H*, *He*, *Li* and *Be* isotopes within the Hauser-Feshbach formalism which takes into account the influence of the total angular momentum of the prefragment. Furthermore, it computes the production of the heavier IMF with the asymmetric splitting of the transition-state model of L.G. Moretto[6]. SMM takes into account the Weisskopf-Ewing evaporation of light IMF and the multifragmentation channels (instantaneous break-up of the prefragment), supposed to play an important role at high excitation energies.

There are two techniques to study experimentally spallation: Either direct kinematics is used, where a proton beam is directed onto an atomic target, or inverse kinematics is chosen, in which case a heavy-ion beam impinges on a proton target. The SPALADIN experiment is based on the use of the inverse kinematics.

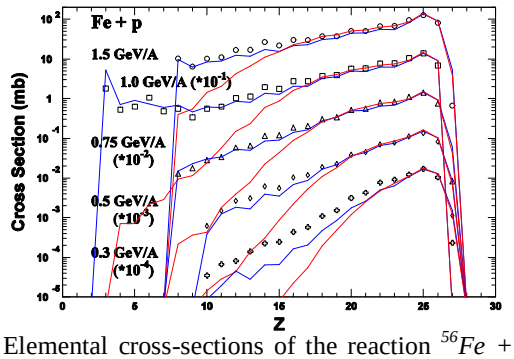

Fig. 1 Elemental cross-sections of the reaction $^{56}Fe + p$ measured at GSI-FRS[8] at five different beam energies, 0.3, 0.5, 0.75, 1.0 and 1.5 *GeV* per nucleon from bottom to top, and compared to GEMINI and ABLA, both coupled to INCL4. ABLA is unable to reproduce the measured cross-sections at low Z for the five values of the beam energy, which is not the case of GEMINI.

There are two advantages to the utilization of inverse kinematics in the study of spallation. The first one is that the low centre-of-mass kinetic energy fragments produced in the reaction are focused in the forward direction with very small angles with respect to the incoming beam direction. Such a focusing, due to the Lorentz boost from the centre-of-mass frame to the laboratory frame, provides a high geometrical efficiency for the detection of these fragments, almost 4 π of solid angle in the centre-of-mass, with detectors of rather limited aperture in the laboratory. The second advantage is that these fragments are essentially emitted with the beam velocity in the laboratory (β ~ 0.87 *c* at 1 *GeV* per nucleon), i.e. at high energy in the laboratory. Such a feature of the kinematics permits an almost threshold-free detection of IMF and spallation residues as well as light particles evaporated from the prefragment. These particles, fragments and residues hardly exit the target in direct kinematics.

The combination of these two properties of inverse kinematics provides a very efficient characterization of the spallation final-state distribution focused on centre-of-mass low-energy fragments. In principle, on an event-by-event basis, all the products coming from the decay of the prefragment can be detected. Hence, a coincidence measurement such as the one presented here performed with SPALADIN provides a full coverage of the phase-space of the prefragment decay.

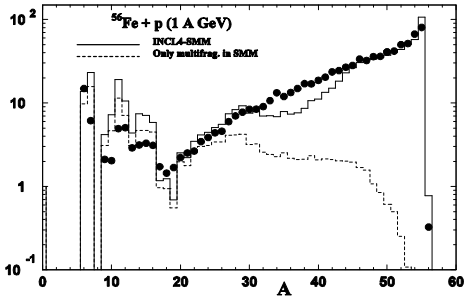

Fig. 2 The isobar production cross-sections (in *mb*) of the reaction $^{56}Fe + p$ at 1 *GeV* per nucleon measured at GSI-FRS[8] and compared to SMM (full line) in which the multifragmentation contribution has been identified (dotted line)

The present work follows an effort of complete and extensive measurements performed at the fragment separator (FRS) of GSI (Darmstadt, Germany) on the detection and identification of heavy residues and fission products in the spallation of different nuclei, from ^{56}Fe to ^{238}U, in an energy range spanning from 0.2 to 1.5 *GeV* per nucleon[8]. With respect to these measurements, a more complete characterization of the final states should permit to distinguish between the different possible mechanisms able to describe the IMF production cross-section in the prefragment decay. It can be seen in Figs. 1 that to reproduce the measured IMF cross-sections, a mechanism beyond the "classical" Weisskopf-Ewing evaporation of *n*, *p* and ^{4}He, as proposed by the ABLA model is necessary. However, these inclusive data are rather well reproduced, though not perfectly by both GEMINI and SMM (coupled to INCL4). Furthermore, as we can see in Fig. 2, the contribution of multifragmentation, totally absent in GEMINI, contributes rather importantly in the cross-section, according to SMM and provides a fair description of the low-Z cross-sections. This has led some to interpret the characteristics of recoil velocity spectra of

IMF in the reaction $^{56}Fe + p$ as a possible indication of the onset of multifragmentation in the reaction[9].

I.B. Experimental set-up

The SPALADIN experimental set-up is shown on Fig. 3. It was installed in GSI. A liquid-hydrogen target was the proton target, of 88.5 ± 2.2 *mg/cm*^{2} thickness. The spallation residues were tracked upstream of the large aperture dipole magnet ALADiN with an ionization chamber (MUSIC, in Fig. 3) for charge identification, high-resolution position detectors (drift chambers) and a Ring Imaging Cerenkov (RICH) for the measurement of their velocities, and downstream in the large time-projection chamber (TP-MUSIC 4). The combination of the ALADiN upstream and downstream information allowed reconstructing the spallation residues' masses and recoil velocities in the rest frame of the ^{56}Fe nucleus. These data were presented at the AccApp'05 conference[10]. The light-charged particles were detected, tracked and identified in the TP-MUSIC 4 and in the time-of-flight wall (hodoscope in Fig. 3) and the neutrons were detected in the high-efficiency Large Acceptance Neutron Detector LAND. The set-up is described in detail in Refs.[10, 11, 12].

The detection efficiencies (ε_{DET}) of the different types of fragments and particles were determined with the recorded data. We have: ε_{DET} = 44 % for *H*, 78 % for *He*, 83 % for *Li* and ≥ 94 % for the heavier fragments. The geometrical efficiencies ε_{GEOM} of the set-up were computed with a complete GEANT 4 (Ref. [13]) simulation, which gave: ε_{GEOM} = 20 % for *H*, 80 % for *He* and almost 100 % for heavier fragments. The set-up efficiency to detect hydrogen isotopes was thus of $\varepsilon_{GEOM} \times \varepsilon_{DET} \approx 9$ %, a rather small value. Hence, we restrict the discussion below to the detection of fragments of charge $Z \geq 2$.

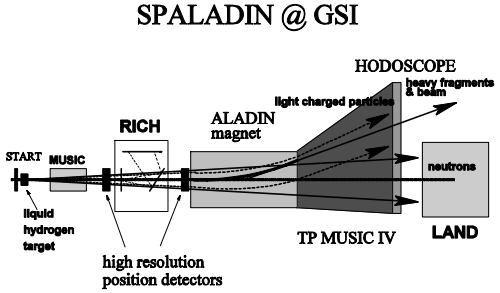

Fig. 3 View of the SPALADIN experimental set-up from the top. The beam comes from the left. The distance between the START detector, on the left of the target, and the LAND detector entrance face is approximately 10 *m*.

II. RESULTS AND DISCUSSION

II.A. Contributions to the total cross-section

Five types of final states have been identified, as shown in Fig. 4 which displays the contributions of these final states to the elemental production cross-sections in the reaction:

- Three or more fragments of charge $Z \geq 3$, called IMF in a general way in the discussion below without any *He* in coincidence.
- Two IMF final states, without any *He*.
- At least two IMF with at least one *He*.
- One fragment with at least one *He*,.
- One fragment only in the final state (no *He*)

Three regions in this elemental cross-sections distribution can be identified: 1) the production of "heavy" residues ($Z \geq 15$) where 90 % at least of the cross-sections is given by the contribution of the evaporation of nucleons, hydrogen isotopes and heliums; 2) the lighter IMF production region ($8 \geq Z \geq 3$) where the direct production, along with evaporation, ends mainly with two- or more-fragment final states; 3) the region in between ($14 \geq Z \geq 9$) which comprises a more equilibrated mixing between evaporation residues and direct IMF production. In particular, it seems that "classical" evaporation plays a smaller role in the IMF direct production.

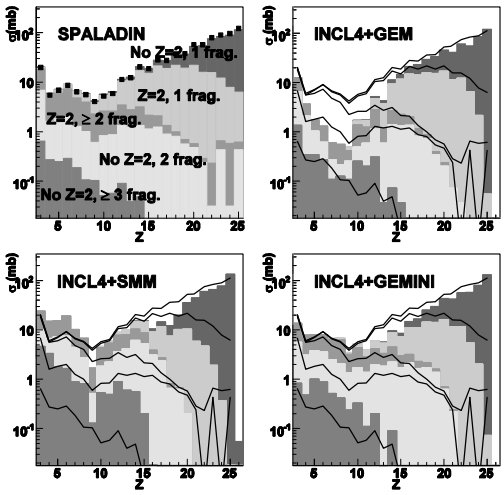

Fig. 4 Identified contributions to the elemental cross-sections in the reaction $^{56}Fe + p$ at 1 *GeV* per nucleon. The SPALADIN data are given in the top-left panel. "frag" means, in this graph, a fragment or residue of charge $Z \geq 3$. These data (the solid curves) are compared in the other panels to three prefragment-decay models coupled to INCL4: GEM, top-right panel; SMM, bottom-left; GEMINI, bottom-right. Note that the model predictions were filtered with the GEANT 4 simulation of

the experimental set-up prior to the comparison with the data.

We have compared our data with GEM, SMM and GEMINI, all three coupled to INCL4. This comparison is displayed in Fig. 4, top-right panel for GEM, bottom-left for SMM and bottom-right for GEMINI. In these three panels, the full curves represent the SPALADIN data of the top-left panel and the histograms represent the model predictions, filtered with the set-up GEANT 4 simulation. This comparison shows that the basic features of the elemental cross-section distribution are rather well described by the three models with the exception of the "intermediate region" ($14 \geq Z \geq 9$) poorly described by GEM which underestimates the measured cross-section by roughly one order of magnitude in this region. The decomposition of the elemental cross-sections into the different identified-final-state contributions shows here its full interest. Indeed, two models' predictions can vary by large factors for a given decay channel even though the agreement on the elemental cross-section can be satisfactory for both. This decomposition exhibits a slightly better description of the *He-* and *H-* and *n-*evaporation-dominated channels by GEM than the two other codes. However, when going towards smaller Z, the overall comparison of these different channels favours GEMINI whose predictions are closer to the data and which ensures a smoother transition from helium-, hydrogen and neutron-evaporation dominated channels to direct fragment-production channels. More specifically, it has to be mentioned that SMM overestimates significantly the multi-fragment channels, especially at the lower Z.

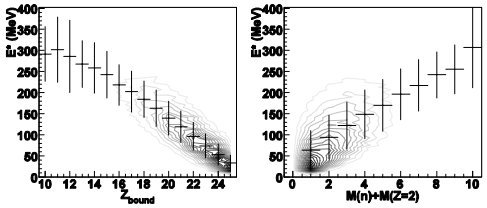

Fig. 5 Excitation energy E^* at the end of the INC versus two experimental observables: Z_{bound} (left) and $M(n) + M(He)$ (right) as computed with the GEANT 4 simulation of the SPALADIN set-up. See text for the definition of these variables.

II.B. Excitation energy determination

In order to understand in greater details this transition from *He-*, *H-* and *n-* evaporation dominated channels of rather low-excitations of the prefragment to the direct production of IMF, which corresponds to higher prefragment excitation energies, we have considered two observables Z_{bound} and $M(n) + M(He)$. The former is the sum of the charges of all the detected products besides the hydrogen isotopes, as proposed for the first time by the ALADiN collaboration[14]; the latter is the sum of the *detected* multiplicities of neutrons and heliums[15]. Using the simulation of the SPALADIN set-up, we could check first that these two variables are correlated to the excitation energy E^* of the prefragment at the end of the INC phase, as shown in Fig. 5. Furthermore, we could also show that these correlations are *independent of the de-excitation model used in the simulation*[12, 13]. This permits a statistical selection of the events in the data according to these two variables in order to study the evolution of the spallation mechanism with E^*.

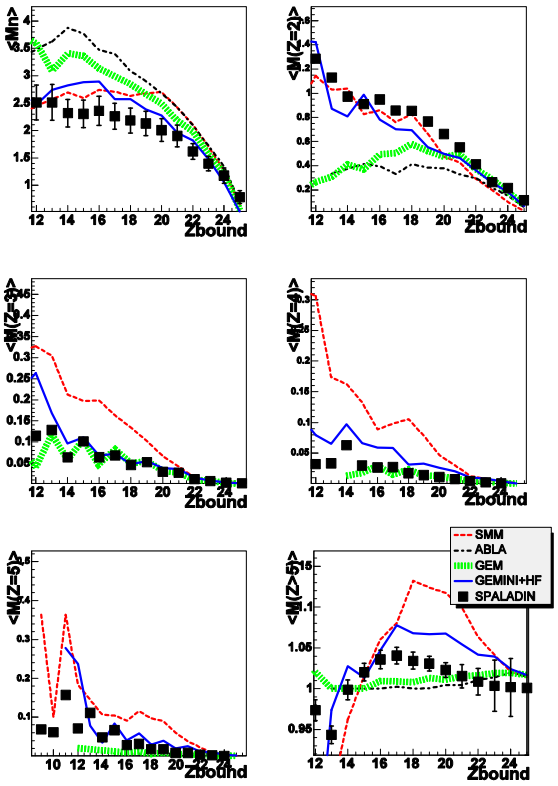

Fig.6 Mean multiplicities of *n*, *He*, *Li*, *Be*, *B* and heavier fragments with Z_{bound} (from top-left to bottom-right). The black squares are the SPALADIN data points, the thick curve is the prediction of GEM, the dashed line is SMM, the dotted line is ABLA and the full thin curve is the GEMINI calculation.

II.C. Evolution of the average multiplicities with the excitation energy

The evolution of the average multiplicities $<M(X)>$ of emitted particles and fragments in the reaction $^{56}Fe + p$ at 1 *GeV* per nucleon with the variable Z_{bound} is shown in Fig. 6 for *n*, *He*, *Li*, *Be*, *B* and heavier fragments. We can see that the trends of the data are well reproduced for *n*

and *He* only by SMM and GEMINI. In particular, the continuous increase of <*M(He)*> with decreasing Z_{bound} is strongly underestimated by both ABLA and GEM which predict a plateau instead. On the other hand, the prediction of GEM is satisfactory for *Li* and *Be* average multiplicities. As we could see when considering the different contributions to the elemental cross-sections, SMM is over predicting the average multiplicities of IMF. Furthermore, a noticeable odd-event effect is present in the <*M(Li)*> and <*M(B)*> SPALADIN data which is nicely explained by GEM and GEMINI. This can be attributed to shell effects, still at play at these rather low excitation energies per nucleon (compared to the average nucleon binding energy), which favours the emission of odd-Z fragments from odd-Z_{bound} prefragments.

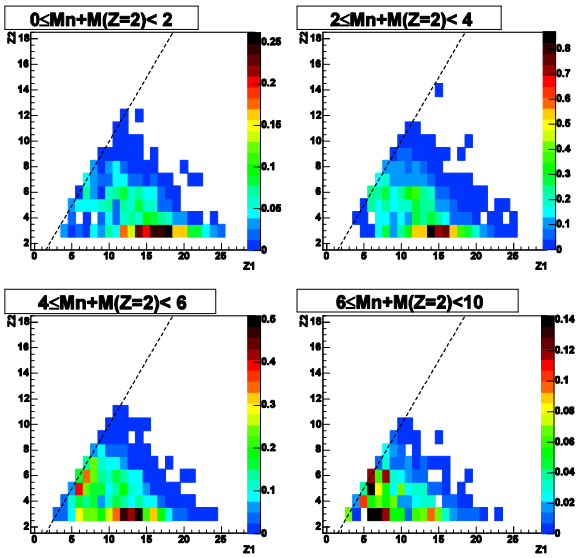

Fig. 7 Multi-fragment (Z ≥ 3) cross-section distributions measured with SPALADIN as a function of Z1 (X-axis), the largest fragment charge of the event and Z2 (Y-axis), the second largest fragment charge in the event. The Z-axis gives the cross-section (scale on the right of each graph, in *mb*) for different selections in *M(n)+M(He)*: [0,1] (top-left), [2,3] (top-right), [4,5] (bottom-left) and [6,9] (bottom-right). The dashed line in the four panels is only here to guide the eye. It corresponds to Z1=Z2.

II.D. Multi-fragments events

In the following, we will focus the data analysis and interpretation on multi-fragments events (Z ≥ 3). These events represent around 7 % of the total cross-section of the reaction ^{56}Fe + *p* at 1 *GeV* per nucleon. In order to probe the evolution of the IMF production mechanism with E^*, we performed a selection of the events with *M(n) + M(He)*. This variable was preferred to Z_{bound} because neutrons and heliums do not contribute to the multiplicities of fragments of charge Z ≥ 3. Using such a selection, as shown in Fig. 7 which represents the cross-section of multi-fragment events (Z-axis of these 2D plots) as a function of Z1, the largest fragment charge in the event (X-axis) and Z2, the second largest fragment charge (Y-axis), we see a clear evolution from asymmetric final states at low *M(n) + M(He)* to an even mixing between rather asymmetric final states to almost identical fragments (Z1 ~ Z2) at the higher values of *M(n) + M(He)*.

In order to be more quantitative and perform a comparison of our data with GEM, SMM and GEMINI, we have plotted, for three ranges of *M(n) + M(He)*, the cross-sections σ(Z1-Z2) in Fig. 8 and σ(Z1+Z2) in Fig. 9

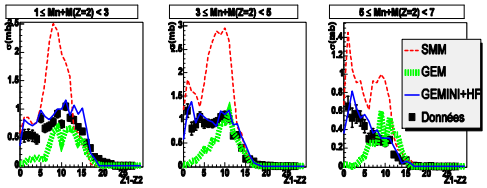

Fig. 8 Cross-section σ(Z1-Z2) (*mb*) for three ranges of *M(n) + M(He)*: [1,2] (left), [3,4] (centre) and [5,7] (right). SMM (dashed curve), GEM (thick dotted curve) and GEMINI (full curve) are coupled to INCL4.

The basic features observed in the 2D plots of Fig. 7 can clearly be seen in these two figures: When going from lower values of *M(n) + M(He)* to higher values, the shape of the cross-section σ(Z1-Z2) is changed from a rather flat Z1-Z2 dependence up to Z1-Z2 ~ 15 to a shape with a clear maximum close to Z1-Z2 = 0. In the same trend, σ(Z1+Z2) has a maximum which drifts to lower values of Z1+Z2 and with a FWHM which increases at the same time. It is remarkable that these features are described coherently by GEMINI only. GEM keeps all over the range of *M(n) + M(He)* selection the same asymmetry in (Z1,Z2) (σ(Z1-Z2) is almost constant) whereas SMM, as seen already, over predicts these cross-sections with the predicted shapes of σ(Z1-Z2) & σ(Z1+Z2) rather poorly describing our data.

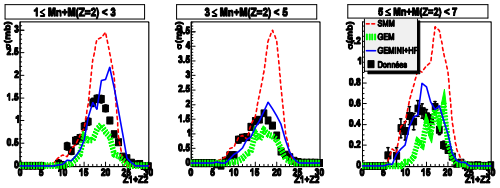

Fig. 9 Cross-section σ(Z1+Z2) (*mb*) for three ranges of *M(n) + M(He)*: [1,2] (left), [3,4] (centre) and [5,7] (right). SMM (dashed curve), GEM (thick dotted curve) and GEMINI (full curve) are coupled to INCL4.

III. CONCLUSION AND OUTLOOK

In the SPALADIN experiment presented here, we apply the inverse kinematics technique to the study of the reaction $^{56}Fe + p$ at 1 *GeV* of proton energy in the centre-of-mass frame (i.e. ~ 1 *GeV* per nucleon of ^{56}Fe beam energy in the laboratory frame). The intrinsic features of this technique permit to detect with both high detection and geometrical efficiencies fragments produced in the reaction with a low kinetic energy in the centre-of-mass frame. This allows measuring absolute cross-sections of multi-fragment and multi-particle final states. We have quantified, with a GEANT 4 simulation, the rather high geometrical efficiencies of our apparatus for all the fragments besides the hydrogen isotopes. Given the fact that in spallation there is mainly one source of such fragments, the prefragment formed at the end of the cascade phase, the measurement in coincidence of these fragments provides a large sensitivity to the prefragment-decay mechanism. We can compare our results almost directly to theoretical predictions for the prefragment decay mechanism.

Using our data and the comparison with four de-excitation codes, ABLA, GEM, SMM & GEMINI coupled to the intranuclear cascade INCL4, we could show that the reaction $^{56}Fe + p$ at 1 *GeV* per nucleon is better described by GEMINI + INCL4 than by the other combinations, in the overall shape of the cross-section as well as in the contribution to the cross-section of the different identified final states (1 or more fragment(s), i.e. of charge $Z \geq 3$, in coincidence or not with *He*). We could show in particular that the production of intermediate-mass fragments (IMF) in this reaction is essentially due to asymmetric splitting and that for the major part of the events having an IMF of charge $Z \leq 9$ in the final state, there are two fragments in coincidence.

Moreover, as we could show with our simulation of the SPALADIN set-up, we have access to experimental observables which allow selecting events in different classes of average excitation energies. We could demonstrate that this selection of events is experimentally meaningful in the sense that it doesn't depend, at the level of sensitivity of our experiment, on the relative importance of the prefragment decay channels. This has to be mainly related to the fact that our experimental set-up is highly efficient with practically the same efficiency to all reaction products from the decay of the excited system heavier than the hydrogen isotopes. This enabled us to study, independently of any intranuclear cascade model, the evolution of the reaction mechanism with the excitation energy of the prefragment.

We have applied this to the detailed study of the IMF production as a function of the excitation energy of the prefragment. This detailed study confirms to a high level of accuracy (with respect to the error bars of the experiment, in the 10 % level) the good description of the reaction by the code GEMINI + INCL4.

We are going in a near future to use the same experimental technique, i.e. inverse kinematics & coincidence measurements in approximately an identical set-up, for two other studies of spallation:

- The study of the reactions $^{28}Si + p$ and $^{136}Xe + p$, Ref.[16]
- The measurement of the fission channels of the spallation of heavy nuclei[17].

Both experiments will be performed at beam energies ranging from 0.5 to 1 *GeV* per nucleon.

The first measurement, S304, will complete the study presented here on the reaction $^{56}Fe + p$ and will provide the mass dependence of the spallation mechanism and of the different reaction channels. This will give also the dependence of the mechanism on the average prefragment excitation energy. In fact, the prefragment excitation energy ranges from 0 to 10 *MeV* per nucleon in the reaction $^{28}Si + p$, from 0 to 7 *MeV* per nucleon in the reaction $^{56}Fe + p$ and remains always below 4 *MeV* per nucleon in the reaction $^{136}Xe + p$.

The second experiment is aiming at measuring in coincidence the fission fragments, the evaporated neutrons and the produced heliums. Such a coincidence detection will allow reconstructing the characteristics of the fissioning system, which is of major importance for the understanding and modelling of fission which occurs in spallation on rather highly excited systems (the prefragment at the end of the intranuclear cascade) as compared with the fission occurring in the Coulomb excitation of heavy fragments or in the absorption of thermal neutrons, in which cases shell effects are much more important.

On a longer term, the SPALADIN collaboration is involved in the R^3B collaboration[18]. This collaboration has in charge the high-energy branch of the secondary-beam facility of the FAIR project at GSI[19]. R^3B is building a new large-aperture superconducting dipole magnet which will increase dramatically the final-state phase-space coverage of the ion reactions in the *GeV* per nucleon range and, in particular, of spallation reactions in inverse kinematics. Using the new magnet and a larger time-projection chamber (TPC) adapted to its dimensions, we will be able to measure with a high geometrical efficiency in coincidence the light fragments, the neutrons and the fission products and heavy residues of the spallation of heavy nuclei such as ^{208}Pb or ^{238}U. As we could compute with a simulation of the future R^3B set-up, ε_{GEOM} will increase from 80 to 95 % for heliums and from 20 to 80 % for protons produced in the reactions[20].

Such an experiment will be a definitive benchmark for theoretical models of spallation, for intranuclear

cascade models as well as for de-excitation codes. Because of the much improved experimental acceptance with respect to the present SPALADIN set-up, we will be able to identify efficiently many different final states of the reaction, each of them, as shown here for the reaction $^{56}Fe + p$, being a test for the models. Furthermore, a more efficient detection of the decay products of the prefragment will allow reconstructing experimental observables strongly correlated to the characteristics of the prefragment in the two-step model: Mass, charge and excitation energy. These observables will provide a sensitive test for the intranuclear cascade models independently of the decay channels of the prefragment. In this respect, the two-step model of spallation will be fully tested within the same data: The INC codes independently of the prefragment decay models, as stated above, and the prefragment decay models independently of any INC model, as we did with the data presented here but with much higher accuracy and resolution on the prefragment characteristics.

ACKNOWLEDGMENTS

We acknowledge the support of the European Union under the contract RII3-CT-2004-506065.

REFERENCES

1. J.-É. Ducret *et al.*, SPALADIN collaboration, proposal S248 to the EA (program advisory committee) of GSI (Dec. 2000).
2. A. Boudard *et al.*, *Physical Review C* **66**, 044615 (2002).
3. A.R. Junghans *et al.*, *Nuclear Physics A* **629**, 635 (1998).
4. S. Furihata *et al.*, *Nuclear Instruments & Methods B* **171**, 251 (2000).
5. R.J. Charity *et al.*, *Nuclear Physics A* **483**, 371 (1988).
6. J.P. Bondorf *et al.*, *Physics Reports* **257**, 133 (1995) and references therein.
7. L.G. Moretto, *Physics Letters B* **40**, 185 (1972), *Nuclear Physics A* **247**, 211 (1975).
8. C. Villagrasa-Canton *et al.*, *Physical Review C* **75**, 044603 (2007).
9. P. Napolitani *et al.*, *Physical Review C* **70**, 054607 (2004).
10. É. Le Gentil *et al.*, *Nuclear Instruments and Methods A* **562**, 743 (2006).
11. É. Le Gentil, Doctorate Thesis, University of Evry, France (2006).
12. J.-É. Ducret, Habilitation Thesis, University of Caen – Basse Normandie (2006).
13. http://cern.ch/geant4.
14. J. Hubele *et al.*, *Zeitschrift für Physik A* **340**, 263 (1991).
15. W. A. Friedman, *Physics Letters B* **242**, 309 (1990).
16. J.-É. Ducret *et al.*, SPALADIN collaboration, proposal 304 to the EA of GSI (2005).
17. A. Boudard *et al.*, SPALADIN collaboration, proposal S293 to the EA of GSI (2005).
18. R^3B: Reaction studies with Relativistic Radioactive Beams, http://www-land.gsi.de/r3b/
19. FAIR: Facility for Antiproton and Ion Research, http://www.gsi.de/fair/.
20. J.-É. Ducret *et al.*, "A programme for the study of nuclear reaction mechanisms in the GeV range", proposal to the scientific committee of DAPNIA/SPhN, CEA-Saclay (Oct. 2006).